Spatio-Temporal Correlation-Based Density Optimization in Wireless Underground Sensor Networks

Zhi Sun and **Ian F. Akyildiz**
Broadband Wireless Networking Laboratory, School of Electrical and Computer Engineering
Georgia Institute of Technology, Atlanta, GA, 30332, United States. Email: {zsun; ian}@ece.gatech.edu

***Abstract*—This paper investigates the optimal sensor density in Wireless Underground Sensor Networks (WUSNs) to guarantee high monitoring accuracy with minimum deployment cost. In WUSNs, the density of underground sensors is expected to be as low as possible due to the high deployment cost. However, an extremely high density of underground sensors is required to maintain the full connectivity of WUSNs due to the harsh underground channel conditions. This conflict constitutes the greatest challenge to deploy the WUSNs and was not addressed before, to our knowledge. In this paper, a spatio-temporal correlation-based data collection scheme is proposed to release the unfeasible sensor density requirement of the full connectivity in WUSNs. More importantly, an explicit solution for sensor density optimization in WUSNs under the proposed data collection scheme is developed such that the effects of the dynamic underground channel conditions, the spatio-temporal correlations, the network connectivity, and the random or controlled mobility of mobile sinks are captured. The results of this paper provide principles and guidelines for the design and deployment of wireless underground sensor networks.**

I. Introduction

Wireless Underground Sensor Networks (WUSNs) consist of wireless sensors buried underground, which enable a wide variety of novel applications, such as intelligent irrigation, border patrol, and underground infrastructure monitoring [1].

Despite the potential advantages, the greatest barrier in designing WUSNs is the conflict between the high deployment cost of underground sensors and the high underground sensor density required to achieve fully connected network. On the one hand, since the deployment and maintenance costs of underground sensors are extremely high compared with terrestrial sensor networks, the sensor density in WUSNs should be minimized. On the other hand, due to the material absorption in soil medium, the communication range between underground sensors is very limited ($\leq$ 5 m) [2]. Consequently, a prohibitively high density of underground sensors is required to guarantee the network connectivity [3], [4].

To address this conflict, one feasible solution is to let the above ground vehicles, people, or some dedicated robots inside the field carry transceiver devices and serve as mobile sinks. The mobile sink either moves randomly (e.g. vehicles and people) or moves under control (e.g. robots). By utilizing the mobile sinks, the WUSNs are not necessary to be fully connected. Due to the reduced connectivity, the WUSNs are divided into multiple unconnected clusters. When a mobile sink moves into the communication range of any underground sensors in one cluster, it can collect the measured data from all the underground sensors in this cluster. By this data collection scheme, the sensor density in WUSNs can be reduced.

† This work was supported by the US National Science Foundation (NSF) under Grant No. CCF-0728889.

However, under this data collection scheme, the mobile sinks cannot collect the data of every sensor at every time stamp due to the not fully connected network. The data at uncollected positions and time stamps needs to be estimated by utilizing the spatio-temporal correlations between the monitored data [6]. Since the wireless underground sensor nodes act not only as sensors but also as data transceivers and relays, the sensor density determines both the spatial and temporal sampling rate. There exists an optimal density of the underground sensors that can achieve satisfying monitoring accuracy with minimum deployment cost.

Finding this optimal sensor density is a complicated due to the unique channel characteristics and the heterogeneous network architecture in WUSNs, which requires a jointly analysis of the three types of communication channels in WUSNs, the spatio-temporal correlations, the network connectivity, and the sink mobility. To the best of our knowledge, this problem has not been addressed by the research community so far.

In this paper, we theoretically investigate the optimal sensor density in WUSNs that can guarantee high monitoring accuracy with minimum sensor deployment cost. Specifically, we introduce a spatio-temporal correlation-based data collection scheme for WUSNs to release the unfeasible sensor density requirement in WUSNs. Then, we present an explicit solution for sensor density optimization in WUSNs under the proposed data collection scheme. To formalize the optimization solution, the upper bound of the monitoring error is calculated as the objective function, which is explicitly expressed as a function of dynamic underground channel model, spatio-temporal correlations, network connectivity, and mobility of mobile sinks. The results of this paper provide principles and guidelines for the design and deployment of WUSNs.

The remainder of this paper is organized as follows. In Section II, the underground channel model is described. In Section III, the spatio-temporal correlation-based data collection scheme is proposed. Next, in Section IV, the optimal sensor density in WUSNs under the proposed data collection scheme is derived. Then, in Section V, numerical studies are performed. Finally, the paper is concluded in Section VI.

II. Underground Channel Characteristics

In this section, we calculate the communication ranges of the three types of channels in WUSNs.

A. Path Loss of UG-UG Channel

The path loss of Underground-to-Underground (UG-UG) channel consists of two parts: the UG path loss L_{UG} and the additional path loss $V_{reflect}$ caused by the reflected second path from the air-ground interface, i.e.

$$L_{UG-UG} = L_{UG}(d_{UG}) + V_{reflect}(d_{depth}) , \quad (1)$$

where the UG path loss L_{UG} is a function of UG path length d_{UG}, operating frequency, soil water content, soil bulk density, and composition of soil in terms of sand and clay fractions; the additional path loss $V_{reflect}$ is a function of all the parameters of L_{UG} plus the burial depth d_{depth} of UG sensors. The expressions of $L_{UG}(d_{UG})$ and $V_{reflect}(d_{depth})$ can be found in [2].

B. Path Loss of UG-AG Channel and AG-UG Channel

The path loss of Underground-to-Aboveground (UG-AG) channel L_{UG-AG} consists of: the UG path loss L_{UG}, the AG path loss L_{AG}, and the refraction loss from soil to air L^R_{UG-AG}, i.e.

$$L_{UG-AG} = L_{UG}(d_{UG}) + L_{AG}(d_{AG}) + L^R_{UG-AG} \ , \tag{2}$$

where d_{UG} is the length of the UG path; d_{AG} is the length of the AG path. Similar to the UG-AG channel, the path loss of the Aboveground-to-Underground (AG-UG) channel is

$$L_{AG-UG} = L_{UG}(d_{UG}) + L_{AG}(d_{AG}) + L^R_{AG-UG} \ , \tag{3}$$

where L^R_{AG-UG} is the refraction loss from air to soil. The AG path loss L_{AG} can be calculated using Friis transmission equation. The detailed expression of the refraction loss L^R_{UG-AG} and L^R_{AG-UG} can be found in [3], [4], which are functions of the soil dielectric properties, the burial depth of UG sensor, the distance between the transceivers, and the antenna height of the AG sink.

C. Transmission Ranges of the Three Types of Channels

If the transmit power is P_t and the antenna gains are g_r and g_t, then the received power $P_r(d)$ at a sensor d meters away is $P_r(d) = P_t+g_r+g_t-L_{path}(d)$, where $L_{path}(d)$ is the corresponding path loss given by (1), (2), or (3). Then the corresponding communication range of the channel can be calculated as

$$R = \max\{d : P_r(d)/P_n > SNR_{th}\} \ , \tag{4}$$

where P_n is the noise power; and SNR_{th} is the minimum signal-to-noise ratio required by the receiver.

We denote the communication range of the UG-UG, UG-AG, and AG-UG channel as R_{UG-UG}, R_{UG-AG}, and R_{AG-UG}, respectively. According to the above models, R_{UG-UG} is the smallest ($\leq$ 5 m). R_{UG-AG} and R_{AG-UG} are in the range of 10 m to 50 m. R_{UG-AG} is larger than R_{AG-UG}, since a large portion of signal energy can penetrate the air-ground interface from soil to air while most energy is reflected back in the opposite direction. However, this difference becomes smaller when the sensor burial depth decreases [5]. The ranges of all the three types of channels decrease dramatically as the soil water content increase. The sensor burial depth has significant influence on R_{UG-AG} and R_{AG-UG}. However, in most applications, the burial depth has little influence on R_{UG-UG}.

III. Spatio-Temporal Correlation-Based Data Collection

In this section, we proposed a spatio-temporal correlation-based data collection scheme in WUSNs. By utilizing the spatio-temporal correlations and the AG mobile sinks, the WUSNs are not necessary to be fully connected so that the UG sensor density can be reduced. When a mobile sink moves into the transmission range of one UG sensor, the communication is initiated by the data request from the mobile sink. This request is then broadcasted by this connected UG sensor to all other UG sensors in the same cluster. Finally, all the UG sensors in this cluster report their measurement data to the mobile sink in a multi-hop fashion. Due to the reduced network connectivity and the usage of mobile sinks, not every UG sensor's data is available at the monitoring center at every time stamp. The time stamp when a certain data is available depends on the network connectivity and the sink mobility. Moreover, not every position in the field has a UG sensor due to the limited sensor density. Since all the monitored data are spatio-temporally correlated, the unavailable data at any interested locations and time stamps can be estimated by the least-squares linear regression (kriging) algorithms [6].

IV. Sensor Density Optimization in WUSNs

In this section, we derive the analytical solution for sensor density optimization in WUSNs.

A. Network Model

The WUSN is deployed in an arbitrary convex 2D region $\mathbb{R}^2$. The UG sensors $\{N_i\}$ are distributed inside $\mathbb{R}^2$ according to a homogeneous Poisson process of intensity λ. The sensor burial depths $\{z_i\}$ are uniformly distributed in $[z_{min}, z_{max}]$. There are m mobile AG sinks $\{M_i\}$ carried by people, machineries, or robots inside region $\mathbb{R}^2$. The movement of those mobile sinks can be either random or under control.

B. Spatio-Temporal Correlation Model

Unavailable data $z(\boldsymbol{x}, t)$ at location $\boldsymbol{x}$ and time stamp t can be estimated by kriging algorithm [6]. If there are n sensors, the unbiased estimation $z^*(\boldsymbol{x}, t)$ is a linear combination of the latest available data of all the n sensors $\{z(\boldsymbol{x}_i, t_i), i = 1, 2, \dots n\}$:

$$z^*_n(\boldsymbol{x}, t) = \textstyle\sum_{i=1}^n \alpha_i \Big[z(\boldsymbol{x}_i, t_i) - \mu\Big] + \mu \ , \tag{5}$$

where $\{\alpha_1, \alpha_2, ..., \alpha_n\}$ are determined to minimize the error variance. Then the minimum error variance is derived:

$$\sigma^2_n = C(0)\Big[1 - \textstyle\sum_{i=1}^n \alpha_i^{opt} \cdot \rho(\boldsymbol{x}_i, \boldsymbol{x}, \Delta t_i)\Big] \ , \tag{6}$$

where $C(0)$ is the variance of the data; $\rho(\boldsymbol{x}_i, \boldsymbol{x}, \Delta t_i)$ is the correlation function between the data at the space-time coordinate $(\boldsymbol{x}_i, t_i)$ and the data at the coordinate $(\boldsymbol{x}, t)$; $\Delta t_i = t - t_i$. The mean, variance, and correlation function of the monitored data can be derived by the spatio-temporal models, which varies from case to case in different applications. In this paper, we use the soil moisture [7], [8] as an example. In this paper, only the correlation function is needed, which is:

$$\rho(\boldsymbol{x}_i, \boldsymbol{x}_j, \Delta t_{ij}) = \frac{\eta e^{-a\Delta t_{ij}} - a e^{-\eta\Delta t_{ij}}}{\eta - a}\left(1 + \frac{r_R d_{ij}}{4}\right) e^{-r_R \frac{d_{ij}}{2}} \ , \tag{7}$$

where a is normalized soil water loss; $1/r_R$ and $1/\eta$ are the mean cell radius and duration of rain/irrigation, respectively; d_{ij} is the distance between the two locations; $\Delta t_{ij} = t_i - t_j$.

C. Optimization Problem Formalization

The optimal sensor density in WUSNs is actually the minimum sensor density that can guarantee a certain level of overall monitoring accuracy. The overall monitoring accuracy in a WUSN is measured by the average error of every position and every time stamp through out the WUSN denoted by $E[\sigma^2]$. Then the density optimization can be formalized as

$$\begin{aligned} Given: &\quad \text{Underground channel and spatio-temporal model,} \\ &\quad \text{Number and mobility model of mobile sinks.} \\ Find: &\quad \min \lambda \\ s.t.: &\quad E[\sigma^2] < \sigma^2_{max}, \end{aligned} \tag{8}$$

where σ_{max}^2 is the maximum tolerable mean error. To solve this optimization problem, we first calculate the objective function $E[\sigma^2]$. Due to the highly random network topology, it is impossible to find out the exact expression of $E[\sigma^2]$. Instead, we use the upper bound of $E[\sigma^2]$ as the new objective function, which can guarantee the required monitoring accuracy.

Notations are described first: t_{now} is the current time stamp; $\{\boldsymbol{a} \leftrightarrow \boldsymbol{b}\}$ denotes that the sensor at position $\boldsymbol{a}$ is connected to the sensor at $\boldsymbol{b}$ by single/multiple hops; $\{\boldsymbol{a} \longleftrightarrow \text{sink at } \Delta t\}$ denotes that, at time stamp $t_{now} - \Delta t$, the sensor at $\boldsymbol{a}$ is connected to a mobile sink for the last time by single/multiple hops; and $\{\boldsymbol{a} \overset{\text{direct}}{\longleftrightarrow} \text{sink at } \Delta t\}$ denotes that, at time stamp $t_{now} - \Delta t$, the sensor at $\boldsymbol{a}$ is directly covered by a mobile sink for the last time. Then the average error is given by

$$E[\sigma^2] = E\left[E[\sigma^2|n \text{ sensors}]\right] = \sum_{n=1}^{\infty} E[\sigma_n^2] \frac{(\lambda S_{\mathbb{R}^2})^n}{n!} e^{-\lambda S_{\mathbb{R}^2}}, \quad (9)$$

where the probability that there are n sensors is calculated according to the Poisson point process; $S_{\mathbb{R}^2}$ is the area of the region $\mathbb{R}^2$; $E[\sigma_n^2]$ is calculated by (6). To avoid calculating the partial derivatives to get the optimal weights $\{\alpha_1^{opt}, \alpha_2^{opt}, ..., \alpha_n^{opt}\}$ in (6), a simple weight setting $\{\alpha_1^*, \alpha_2^*, ..., \alpha_n^*\}$ is used to calculate the upper bound of the error variance, where $\alpha_i^* = 1$ if $\boldsymbol{x}_i$ is the closest to $\boldsymbol{x}$ among the n sensors, otherwise $\alpha_i^* = 0$. This setting is equal to the widely used strategy that the data at the closest sensor is utilized. Then

$$E[\sigma_n^2] \quad (10)$$
$$\leq 2C(0)\left\{1 - E\Big[\rho(\boldsymbol{x}_i, \boldsymbol{x}, \Delta t_i)\Big|\boldsymbol{x}_i \text{ is closest to } \boldsymbol{x}, i \in \{1, ..., n\}\Big]\right\} .$$

We first define three events as follows:

- A : One of the n sensors is located at $\boldsymbol{x}'$;
- B : This sensor $\longleftrightarrow$ sink at $\Delta t \leq \Delta t'$;
- C : This sensor is closest to $\boldsymbol{x}$ than any other n–1 sensors.

Then,

$$E\Big[\rho(\boldsymbol{x}_i, \boldsymbol{x}, \Delta t_i)\Big|\boldsymbol{x}_i \text{ is closest to } \boldsymbol{x}, i \in \{1, ..., n\}\Big] \quad (11)$$
$$\geq E\Big[\rho(\boldsymbol{x}', \boldsymbol{x}, \Delta t')\Big|A, B, C\Big]$$
$$= \int_{\boldsymbol{x}\in\mathbb{R}^2} \frac{1}{S_{\mathbb{R}^2}} \int_0^{\Delta t_{max}} \frac{1}{\Delta t_{max}} \int_{\boldsymbol{x}'\in\mathbb{R}^2} \rho(\boldsymbol{x}', \boldsymbol{x}, \Delta t')\, f_{\boldsymbol{x}'}(A,B,C)\; d\boldsymbol{x}\, d\boldsymbol{x}'\, d\Delta t' ,$$

where Δt_{max} is the maximum usable time deviation, i.e. for $\Delta t > \Delta t_{max}$, the temporal correlation is very small.

The probability density function (pdf) of the conditions $\{A, B, C\}$ can be calculated as

$$f_{\boldsymbol{x}'}(A,B,C) = f_{\boldsymbol{x}'}(A) \cdot P(C|A) \cdot P(B\,|\,A,C) , \quad (12)$$

where

$$f_{\boldsymbol{x}'}(A) = n\frac{1}{S_{\mathbb{R}^2}} , \quad P(C|A) = \Big(1 - \frac{S_{\mathbb{C}^2\cap\mathbb{R}^2}}{S_{\mathbb{R}^2}}\Big)^{n-1} ,$$
$$P(B\,|\,A,C) \simeq P(B_0') + [1 - P(B_0')] \cdot (n-1) \cdot P(B_i') , \quad (13)$$

where $\mathbb{C}^2$ is the circular region centered at $\boldsymbol{x}$ with radius $d_{xx'} = \|\boldsymbol{x}' - \boldsymbol{x}\|$; $S_{\mathbb{C}^2\cap\mathbb{R}^2}$ is the area of the joint region of $\mathbb{C}^2$ and $\mathbb{R}^2$; event B_0' and B_i' are defined as

- B_0' : $\boldsymbol{x}' \overset{\text{direct}}{\longleftrightarrow}$ sink at $\Delta t \leq \Delta t'$;
- B_i' : $\boldsymbol{x}' \longleftrightarrow \boldsymbol{x}_S^i$ not via relay sensors inside region $\mathbb{C}^2$, and $\boldsymbol{x}_S^i \overset{\text{direct}}{\longleftrightarrow}$ sink at $\Delta t \leq \Delta t'$,

where $\{\boldsymbol{x}_S^1, \boldsymbol{x}_S^2, ..., \boldsymbol{x}_S^{n-1}\}$ are the positions of the other $n-1$ sensors. By substituting (10)-(13) into (9) and using the identical equation $\sum_{n=0}^{\infty} \frac{\lambda^n}{n!} e^{-\lambda} \equiv 1, \forall\lambda$, we derive:

$$E[\sigma^2] \leq 2C(0)\Big\{1 - E[\text{closest } \rho]\Big\} , \quad (14)$$

where

$$E[\text{closest } \rho] \geq \frac{\lambda}{\Delta t_{max} S_{\mathbb{R}^2}} \iiint_{\substack{\boldsymbol{x}, \boldsymbol{x}'\in\mathbb{R}^2 \\ \Delta t'\in[0,\Delta t_{max}]}} \rho(\boldsymbol{x}', \boldsymbol{x}, \Delta t') \cdot e^{-\lambda S_{\mathbb{C}^2\cap\mathbb{R}^2}} \quad (15)$$
$$\cdot \Big\{P(B_0') + \lambda \cdot (S_{\mathbb{R}^2} - S_{\mathbb{C}^2\cap\mathbb{R}^2}) \cdot [1 - P(B_0')] \cdot P(B_i')\Big\} \cdot d\boldsymbol{x} d\boldsymbol{x}' d\Delta t' ,$$

where

$$P(B_0') = P(\boldsymbol{x}' \overset{\text{direct}}{\longleftrightarrow} \text{sink at } \Delta t \leq \Delta t') , \quad (16)$$
$$P(B_i') = \frac{1}{S_{\mathbb{R}^2} - S_{\mathbb{C}^2\cap\mathbb{R}^2}} \int_{\boldsymbol{x}_S\in\mathbb{R}^2-\mathbb{C}^2} P(\boldsymbol{x}_S \overset{\text{direct}}{\longleftrightarrow} \text{sink at } \Delta t \leq \Delta t')$$
$$\cdot P(\boldsymbol{x}' \leftrightarrow \boldsymbol{x}_S \text{ not via } \mathbb{C}^2)\, d\boldsymbol{x}_S , \quad (17)$$

where $P(\boldsymbol{x}' \leftrightarrow \boldsymbol{x}_S \text{ not via } \mathbb{C}^2)$ is the probability that the sensor at $\boldsymbol{x}'$ is connected to the other sensor at $\boldsymbol{x}_S$ without using relay sensors inside region $\mathbb{C}^2$.

According to (14) and (15), the upper bound of the average monitoring error $E[\sigma^2]$ is determined by the correlation function $\rho(\boldsymbol{x}_i, \boldsymbol{x}_j, \Delta t_{ij})$ in (7) and the probabilities $P(B_0')$ and $P(B_i')$ in (16) and (17). To calculate $P(B_0')$ and $P(B_i')$, two probabilities, $P(\boldsymbol{x}' \leftrightarrow \boldsymbol{x}_S \text{ not via } \mathbb{C}^2)$ and $P(\boldsymbol{y} \overset{\text{direct}}{\longleftrightarrow} \text{sink at } \Delta t \leq \Delta t')$ need to be analyzed, where $\boldsymbol{y} = \boldsymbol{x}'$ or $\boldsymbol{x}_S$. Hence, the sensor density optimization problem is decomposed into a network connectivity probability analysis on $P(\boldsymbol{x}' \leftrightarrow \boldsymbol{x}_S \text{ not via } \mathbb{C}^2)$ and a sink mobility analysis on $P(\boldsymbol{y} \overset{\text{direct}}{\longleftrightarrow} \text{sink at } \Delta t \leq \Delta t')$.

D. Network Connectivity Analysis

Proposition 1: The lower bound of the probability that a UG sensor located at $\boldsymbol{x}'$ is connected to another UG sensor located at $\boldsymbol{x}_S$ by single or multi-hops without using the relay nodes inside the circular region $\mathbb{C}^2$ is given by

$$P(\boldsymbol{x}' \leftrightarrow \boldsymbol{x}_S \text{ not via } \mathbb{C}^2) \geq \Big(1 - e^{-\frac{2}{5}\lambda R_{UG-UG}^2}\Big)^{\epsilon(\boldsymbol{x}', \boldsymbol{x}_S, \boldsymbol{x})} , \quad (18)$$

where R_{UG-UG} is the communication range of the UG-UG channel that is derived in Section II; the detailed expression of the function $\epsilon(\boldsymbol{x}', \boldsymbol{x}_S, \boldsymbol{x})$ is given in the proof. □

Proof: We use similar strategy we developed in [3], [4] to prove this proposition. As shown in Fig. 1, we first map the WUSN on a lattice L (plain) and its dual L' (dashed). The vertices of L' are placed in the center of every square of L. The edges of L' cross every edge of L. Hence, there exists a one-to-one relation between the edges of L and L'. L and L' have the same edge length $d = \frac{1}{\sqrt{5}} R_{UG-UG}$. The edge length is designed so that two UG sensors deployed in two adjacent squares of the lattice L are guaranteed to be connected to each other. One vertex of the dual lattice is located at $\boldsymbol{x}'$. An edge

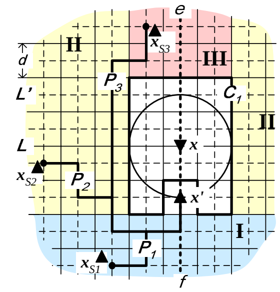

Fig. 1. Mapping the WUSN on a lattice L (plain) and its dual L' (dashed).

l of the L is said to be open if both squares adjacent to l contains at least one UG sensor. An edge l' of the L' is said to be open if and only if the corresponding edge of L is open. A path of the L or $L's$ is said to be open (closed) if all edges forming the path are open (closed).

If there is an open path of L' connecting the two squares in L where $\boldsymbol{x}$ and $\boldsymbol{x}_S$ are located, these two sensors are guaranteed to be connected. The set of all open paths connecting $\boldsymbol{x}$ and $\boldsymbol{x}_S$ without using the relay nodes inside region $\mathbb{C}^2$ is denoted as $\{P_i^o, i = 1, 2, ...\}$, then

$$P(\boldsymbol{x}' \leftrightarrow \boldsymbol{x}_S \text{ not via } \mathbb{C}^2) = P\Big(\cup_i^{\infty} P_i^o\Big) \geq P(P_i^o)\ , \tag{19}$$

where the probability of a certain open path $P(P_i^o)$ is used as the lower bound of $P(\boldsymbol{x}' \leftrightarrow \boldsymbol{x}_S \text{ not via } \mathbb{C}^2)$. To maximize the lower bound, the shortest open path is selected. Hence, the probability of the shortest open path in L' connecting $\boldsymbol{x}'$ and $\boldsymbol{x}_S$ is calculated as the lower bound of $P(\boldsymbol{x}' \leftrightarrow \boldsymbol{x}_S \text{ not via } \mathbb{C}^2)$:

$$P(\boldsymbol{x}' \leftrightarrow \boldsymbol{x}_S \text{ not via } \mathbb{C}^2) \geq (1-q)^{\epsilon(\boldsymbol{x}', \boldsymbol{x}_S, \boldsymbol{x})+1}\ , \tag{20}$$

where $\epsilon(\boldsymbol{x}', \boldsymbol{x}_S, \boldsymbol{x})$ is the length of the shortest open path connecting $\boldsymbol{x}'$ and $\boldsymbol{x}_S$; q is the probability that no sensor exists in a certain square:

$$q = P(\text{No sensor in a square}) = e^{-\frac{1}{5}\lambda R_{UG-UG}^2}\ . \tag{21}$$

The shortest open path may not be a simple straight line since relay nodes can not be inside region $\mathbb{C}^2$. As shown in Fig. 1, a rectangular circuit C_1 is set up so that if the open path does not via the squares inside C_1, the relay nodes along the open path are guaranteed to be outside of circular region $\mathbb{C}^2$. The width and length of the rectangular circuit C_1 are $w_c d$ and $l_c d$, respectively, where

$$w_c = \left\lceil \frac{2\sqrt{5} d_{xx'}}{R_{UG-UG}} + 0.5 \right\rceil, \quad l_c = 2\left\lceil \frac{\sqrt{5} d_{xx'}}{R_{UG-UG}} - 0.5 \right\rceil + 1, \tag{22}$$

where $\lceil a \rceil$ means rounding a to the nearest integer $\geq a$; $d_{xx'} = \|\boldsymbol{x}' - \boldsymbol{x}\|$ is the distance between $\boldsymbol{x}'$ and $\boldsymbol{x}$, which is the radius of region $\mathbb{C}^2$. Construct a new Cartesian coordinate by setting $\boldsymbol{x}'$ as the origin, ef as the y-axis ($\boldsymbol{x}$ is on the positive of y-axis). The new coordinate of $\boldsymbol{x}_S$ is $(x_S^{\text{new}}, y_S^{\text{new}})$. As shown in Fig. 1, the possible positions of $\boldsymbol{x}_S$ are divided into three regions. In different regions, the shortest path connecting $\boldsymbol{x}'$ and $\boldsymbol{x}_S$ is different, e.g. path P_1, P_2, and P_3 in Fig. 1. The length of the shortest path is $\epsilon(\boldsymbol{x}', \boldsymbol{x}_S, \boldsymbol{x})$, and

$$\epsilon(\boldsymbol{x}', \boldsymbol{x}_S, \boldsymbol{x}) \tag{23}$$
$$= \begin{cases} \left\lceil \frac{\sqrt{5}\,|x_S^{\text{new}}|}{R_{UG-UG}} \right\rceil_{rnd} + \left\lceil \frac{\sqrt{5}\,|y_S^{\text{new}}|}{R_{UG-UG}} \right\rceil_{rnd}, & \text{if } \boldsymbol{x}_S \in \text{Region I} \\ 2 + \left\lceil \frac{\sqrt{5}\,|x_S^{\text{new}}|}{R_{UG-UG}} \right\rceil_{rnd} + \left\lceil \frac{\sqrt{5}\,|y_S^{\text{new}}|}{R_{UG-UG}} \right\rceil_{rnd}, & \text{if } \boldsymbol{x}_S \in \text{Region II} \\ l_c + 3 - \left\lceil \frac{\sqrt{5}\,|x_S^{\text{new}}|}{R_{UG-UG}} \right\rceil_{rnd} + \left\lceil \frac{\sqrt{5}\,|y_S^{\text{new}}|}{R_{UG-UG}} \right\rceil_{rnd}, & \text{if } \boldsymbol{x}_S \in \text{Region III} \end{cases},$$

where $\lceil a \rceil_{rnd}$ means rounding a to the nearest integer; Region I: $y_S^{\text{new}} \leq -\frac{1}{2}d$; Region II: $y_S^{\text{new}} > -\frac{1}{2}d$ and $|x_S^{\text{new}}| \geq \frac{1}{2}l_c d$; Region III: $y_S^{\text{new}} > (w_c - \frac{1}{2})d$ and $|x_S^{\text{new}}| < \frac{1}{2}l_c d$. Since $\boldsymbol{x}_S$ cannot appear inside the circuit C_1, there is only one undiscussed region for $\boldsymbol{x}_S$: the square in L that contains $\boldsymbol{x}'$, where $\epsilon(\boldsymbol{x}', \boldsymbol{x}_S, \boldsymbol{x}) \equiv 0$. Finally, substituting (23) into (20) completes the proof. ∎

E. Sink Mobility Analysis

In this subsection, we analyze the random and controlled mobility of the AG mobile sinks to derive the probability $P(\boldsymbol{y} \overset{\text{direct}}{\longleftrightarrow} \text{sink at } \Delta t \leq \Delta t')$ in (16) and (17). Due to the query-based data collection scheme, the effective communication range of the mobile sink is R_{AG-UG} given in Section II.

1) Random Sink Mobility: The mobility of people and vehicles carrying the mobile sinks can be modeled by the widely used Random Waypoint (RWP) Model [10]. In RWP model, the random movement of a node is defined by a sequence of steps consisting of a flight followed by a pause. In each flight, the destination is selected uniformly in region $\mathbb{R}^2$. The speed v and the pause τ are chosen uniformly from $[v_{min}, v_{max}]$ and $[0, \tau_{max}]$, respectively. The lower bound of the probability $P(\boldsymbol{y} \overset{\text{direct}}{\longleftrightarrow} \text{sink at } \Delta t \leq \Delta t')$ under the RWP model has been derived by our work [4]. Hence, we have:

Proposition 2: Given m mobile sinks in region $\mathbb{R}^2$, at time stamp $t_{now} - \Delta t$, the sensor at coordinate $\boldsymbol{y}$ is directly covered by a mobile sink for the last time. Then, the probability that $\Delta t \leq \Delta t'$ is lower bounded by

$$P(\boldsymbol{y} \overset{\text{direct}}{\longleftrightarrow} \text{sink at } \Delta t \leq \Delta t') \geq 1 - \gamma^{\lfloor \frac{\Delta t'}{t_D} \rfloor}\ , \tag{24}$$

where γ and t_D are determined by the AG-UG range R_{AG-UG}, the size of the field $\mathbb{R}^2$, and the RWP model. The detailed expressions of γ and t_D can be found in [4]. □

2) Controlled Sink Mobility: Since the randomly moving sinks are inefficient to collect data, dedicated robots can be employed to improve the data collection efficiency. We adopt the most straightforward strategy to control the multiple robots: The whole region $\mathbb{R}^2$ is divided into m subregions with equal area. Each robot moves inside one of the m subregions with fixed loop route covering the whole subregion. In each subregion, the loop route with minimum length l_{route} is designed for each sink to cover every position.

$$l_{route} \leq \frac{S_{\mathbb{R}^2}/m}{R_{AG-UG}(z_{max})}\ . \tag{25}$$

where $R_{AG-UG}(z_{max})$ is the communication range of AG-UG channel when the sensor is buried at the maximum depth.

Assuming that all the mobile sinks move at a constant velocity v_{robot} without pause. Then the time duration for a sink to complete one loop route in the subregion is $T_{route} = l_{route}/v_{robot}$. That means the UG sensor at any position inside the monitored region can be covered by a sink at least once in every period T_{route}. Therefore, for controlled AG sinks,

$$P(\boldsymbol{y} \overset{\text{direct}}{\longleftrightarrow} \text{sink at } \Delta t \leq \Delta t') \tag{26}$$
$$\begin{cases} \geq \frac{\Delta t'}{T_{route}} \geq \frac{\Delta t' m\, v_{robot}\, R_{AG-UG}(z_{max})}{S_{\mathbb{R}^2}}\ , & \text{if } 0 \leq \Delta t' < \frac{S_{\mathbb{R}^2}}{m\, v_{robot}\, R_{AG-UG}(z_{max})} \\ = 1\ , & \text{otherwise} \end{cases}.$$

F. Sensor Density Optimization Solution

Substituting (18), (24), and (26) into (14)-(17) yields the upper bound of the average monitoring error in WUSNs with random or controlled sink mobility, which is denoted as $\overline{E}[\sigma^2]$. Then, the optimal sensor density in WUSNs with random or controlled sink mobility is derived:

$$\lambda^{opt} = \min\left\{\lambda : \overline{E}[\sigma^2] > \sigma_{max}^2\right\}\ . \tag{27}$$

V. Numerical Analysis

In this section, we numerically analyze the effects of multiple system configurations and environmental conditions in WUSNs. Except studying the effect of certain parameters,

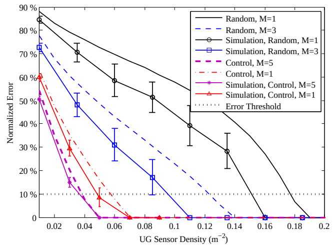

Fig. 2. Normalized monitoring error as a function of the sensor density.

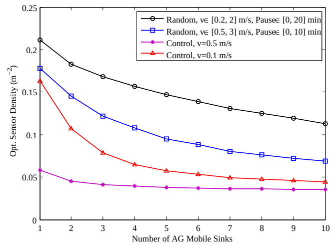

Fig. 3. Optimal sensor density as a function of the mobile sink number.

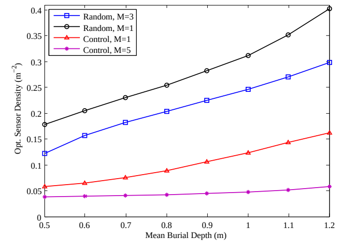

Fig. 4. Optimal sensor density as a function of the mean burial depth.

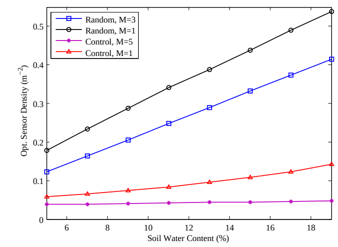

Fig. 5. Optimal sensor density as a function of the soil water content.

default values are set as follows: The monitored region is a $100\ m \times 100\ m$ square. The UG sensors are deployed according to a Poisson point process with intensity λ. The burial depths are uniformly distributed in the interval $[0.3, 0.7]$ m. For the randomly moving sinks, the velocity of each flight is uniformly chosen from $[0.5, 3]$ m/s. The pause duration is uniformly chosen from $[0, 5]$ min. For the controlled robots, the constant moving velocity is set to be 0.5 m/s. The transmitting power is 10 mW at 900 MHz. The minimum received power for correct demodulation is -90 dBm. The antenna height of the AG mobile sinks is 1 m. The mean volumetric water content (VWC) in the soil is 5%. The normalized soil water loss $a = 20$ /day. The irrigation cell radius $1/r_R = 5$ m and the irrigation duration $1/\eta = 60$ sec. The monitoring error is represented by the normalized error, which is calculated by $E[\sigma^2_{norm}] = E(\sigma^2)/C(0)$. The normalized maximum tolerable error $(\sigma^2_{max})_{norm}$ is set as 10%. Each simulation result is averaged over 500 iterations.

In Fig. 2, the theoretical bound of the monitoring error derived in Section IV is validated by simulations. It shows that the error bound is tight enough to serve as the optimization objective function under various system configurations. The optimal sensor density can be read from Fig. 2 by checking the x-coordinate of the intersection point of the error upper bound and the error threshold.

In Fig. 3, the effect of the number and mobility of mobile sinks on the optimal sensor density is captured. Both random and controlled mobility models with different velocities and pause times are considered. It indicates that the optimal sensor density can be significantly reduced by three ways: 1) introducing more mobile sinks, 2) increasing the sink velocity and reducing the pause time, and 3) employing controlled mobile sink instead of the randomly moving sinks. Note that when the moving velocity of the controlled mobile sink is high, the effect of the number of mobile sinks is not obvious since the data collection efficiency is already high enough.

The effects of the sensor burial depth and soil water content are analyzed in Fig. 4 and Fig. 5, respectively. In Fig. 4, the optimal sensor density is give as a function of the mean burial depth. When changing the mean burial depth, we assume that the span of the random depths remains the same, which is 0.4 m. In Fig. 5, the optimal sensor density is given as a function of mean volumetric soil water content. As discussed in Section II, the communication ranges of the three types of channels in WUSNs significantly decrease as the UG sensor burial depth and the soil water content increase. Therefore, the optimal sensor densities of WUSNs dramatically increase as the mean burial depth or the soil water content increases.

VI. Conclusions

The harsh and dynamic underground channel conditions cause prohibitively high density of UG sensors to achieve fully connected networks, which results in extremely high deployment/maintenance cost in WUSNs. In this paper, we first proposed a spatio-temporal correlation-based data collection scheme to release the unfeasible sensor density requirement of the full connectivity in WUSNs. More importantly, we provide an explicit solution for the sensor density optimization in WUSNs under the proposed data collection scheme, which can guarantee the overall monitoring accuracy with minimum deployment/maintenance cost. To formalize the optimization solution, the dynamic underground channel conditions, the spatio-temporal correlation, the network connectivity, and the random or controlled mobility of mobile sinks are jointly analyzed. Our optimization solution clearly captures the effects of multiple system and environmental parameters, including the the number and mobility of the mobile sinks, sensor burial depth, the soil water content, and the spatio-temporal model of the monitored physical quantity. The developed optimization solution provides a flexible tool to determine the optimal sensor density for different application requirements and environmental conditions in WUSNs.

References

[1] I. F. Akyildiz and E. P. Stuntebeck, "Wireless underground sensor networks: Research challenges," *Ad Hoc Networks Journal (Elsevier)*, vol. 4, pp. 669-686, July 2006.

[2] I. F. Akyildiz, Z. Sun, and M. C. Vuran, "Signal Propagation Techniques for Wireless Underground Communication Networks," *Physical Communication Journal (Elsevier)*, Vol. 2, No. 3, pp.167-183, September 2009.

[3] Z. Sun and I. F. Akyildiz, "Connectivity in Wireless Underground Sensor Networks," in *Proc. IEEE SECON '10*, Boston, USA, June 2010.

[4] Z. Sun, I. F. Akyildiz, and G. P. Hancke, "Dynamic Connectivity in Wireless Underground Sensor Networks," submitted to *IEEE Transactions on Wireless Communications*, in March 2011, revised in July 2011. $http://users.ece.gatech.edu/zsun/publications/D\_connectivity\_11$.

[5] A. R. Silva and M. C. Vuran, "Communication with Aboveground Devices in Wireless Underground Sensor Networks: An Empirical Study," in *Proc. IEEE ICC '10*, Cape Town, South Africa, May 2010.

[6] P. Goovaerts, *Geostatistics for Natural Resources Evaluation*, New York: Oxford University Press, 1997.

[7] V. Isham, et.al., "Representation of Space-time Variability of Soil Moisture," in *Proc. Royal Society*, vol.461, no. 2064, pp. 4035-4055, 2005.

[8] X. Dong and M. C. Vuran, "Spatio-temporal Soil Moisture Measurement with Wireless Underground Sensor Networks," in *Proc. IFIP Med-Hoc-Net '10*, Juan-les-pins, France, June 2010.

[9] A. Silva and M. C. Vuran, "Development of a Testbed for Wireless Underground Sensor Networks," *EURASIP Journal on Wireless Communications and Networking*, vol. 2010, Article ID 620307, 2010.

[10] E. Hyytia, P. Lassila and J. Virtamo, "Spatial Node Distribution of the Random Waypoint Mobility Model With Applications," *IEEE Trans. on Mobile Computing*, Vol. 5, No. 6, pp. 680-694, June 2006.